# Silicon-Vacancy Nanodiamonds as High Performance Near-Infrared Emitters for Live-Cell Dual-Color Imaging

*Weina Liu†∇ǂ, Anna Ermakova†⊥*, Yan Liu§, Viatcheslav N. Agafonov⊥, Haoyuan Qi∥, Kaloian Koynov†, Valery A. Davydov#, Rustem Uzbekov○+, Ute Kaiser∥, Theo Lasser†, Fedor Jelezko§*, Tanja Weil†∇**

†Max-Planck-Institute for Polymer Research, Ackermannweg 10, 55128 Mainz, Germany

∇Institute of Inorganic Chemistry I, Ulm University, Albert-Einstein-Allee 11, 89081 Ulm, Germany

ǂInstitute of Materials, École Polytechnique Fédérale de Lausanne, Station 12, 1015 Lausanne, Switzerland

⊥Institute for Physics, Johannes Gutenberg University Mainz, Staudingerweg 7, 55128 Mainz, Germany

§Institute for Quantum Optics, Ulm University, Albert-Einstein-Allee 11, 89081 Ulm, Germany

⊥GREMAN, UMR CNRS-7347, Université de Tours, 37200, Tours, France

‖Central Facility for Electron Microscopy, Ulm University, Albert-Einstein-Allee 11, 89081 Ulm, Germany

#L.F. Vereshchagin Institute for High Pressure Physics, The Russian Academy of Sciences, Troitsk, Moscow, 108840, Russia

○Laboratoire Biologie Cellulaire et Microscopie Electronique, Faculté de Médecine, Université François Rabelais, 37032 Tours, France

+Faculty of Bioengineering and Bioinformatics, Moscow State University, 119992, Leninskye gory 73, Moscow, Russia

KEYWORDS. Nanodiamond, silicon vacancy color center, near infrared cellular imaging, live cell particle tracking.

ABSTRACT. Intracellular imaging is limited by a short bleaching time of fluorescent molecules and particles. In our work we used nanodiamonds with silicon-vacancy centers (SiV) obtained by high-pressure high-temperature synthesis based on metal-catalyst-free growth. They are coated with a polypeptide biopolymer that allows efficient cellular uptake. Our results demonstrate that high photostability and narrow emission in the near-infrared region of nanodiamonds with SiV allow live-cell dual-color imaging and intracellular tracking. Such a system has broad potential applications, which is not limited to live-cell bioimaging, but also include diagnostic (SiV as a nanosized thermometer) and theranostic (nanodiamonds as drug carrier).

Currently, fluorescent molecules are mostly used as labels for intracellular imaging. However, their applications are limited by a fast bleaching time, which makes them ineffective for long-term monitoring. A promising alternative are nanodiamonds (NDs) with color centers that demonstrate high photostability.[1] Depending on the type of color center they can be used for bioimaging and sensing applications, such as super-resolution imaging and nanoscale magnetic field and temperature sensing.[2-4] The most investigated diamond color center is the nitrogen-vacancy center (NV), which consists of a substitution nitrogen atom next to a vacancy. The NDs with NV (ND-NV) are commercially available and can be produced in different sizes and with varying numbers of NVs.[5] NV can be in two charge states: neutral ($NV^0$) or negative ($NV^-$); both have stable fluorescence, but only $NV^-$ is suitable for sensing application.[6] Zero phonon lines (ZPL) of $NV^0$ and $NV^-$ are accompanied by broad phonon sidebands, leading to broad fluorescence emission spanning from ~575 nm to 800 nm.[6] Although ND-NV can be used for long-term monitoring, their fluorescence spectrum partly overlaps with many other optical markers and the cell background so that dual/multicolor imaging remains challenging. In contrast, NDs with negatively charged silicon-vacancy centers (SiV) have recently received considerable attention as potential high-performance bioimaging probes due to their attractive optical properties. [7] In the diamond lattice, the silicon (Si) atom with its larger size compared to carbon replaces two carbon atoms and is located between these two vacancies (Figure 1b). This divacancy structure of the center possesses the inversion symmetry resulting in low sensitivity to strain and contributes to a narrowing of the optical emission.[7] Due to the low electron-phonon coupling, more than 70% of the SiV emission is dominated by the sharp ZPL at ~738 nm with the full width at half maximum of approximately 4 nm.[7] In this way, the emission of NDs containing SiV (ND-SiV) is in the near-infrared (NIR) range (> 700 nm) allowing a deeper tissue penetration and *in vivo* optical

imaging.[8,9] Moreover, the peak position of SiV ZPL has a temperature signature, which is linearly correlated to temperature changes in the range of 295 ± 5 K with sub-kelvin sensitivity.[10] The combination of NIR emission, narrow bandwidth, high photo- and chemical stability, and temperature-dependent ZPL[11,–12] renders ND-SiV as promising candidates for bioimaging and temperature sensing applications in life sciences.

In this work, we report the production and functionalization of ND-SiV for live-cell dual-color imaging and tracking. We optimized the metal-catalyst-free high-pressure high-temperature (HPHT) approach to synthesize ND-SiV with radii of about 50 nm and without the presence of NV centers. The ND-SiV surface was coated by a protein-derived biopolymer based on multiple electrostatic interactions resulting in nanoparticles with enhanced colloidal stability. These coated ND-SiV showed a good uptake by HeLa cells based on an endocytosis mechanism. For the first time, HPHT ND-SiV were used for live-cell dual-color imaging based on their NIR emission, high photostability, and sharp ZPL.

Traditionally NDs are synthesized by HPHT growth in the presence of transition metal catalysts or chemical vapor deposition (CVD) growth.[13] The color centers can be created by adding impurities during diamond growth or by ion implantation. The metal-catalyst-free synthesis is more preferable for fluorescent NDs production since metal atoms can introduce additional defects into the crystal structure and deteriorate color center properties. Such a method is based on the conversion of organic and heteroorganic solids into diamond.[14,15] This technique allows controlling NDs sizes as well as the concentration of the color centers.[16,17] In our work, ND-SiV were produced from a homogeneous mixture of naphthalene ($C_{10}H_8$, Chemapol), octafluoronaphthalene ($C_{10}F_8$, Alfa Aesar), detonation NDs (3-4 nm, SkySpring), and tetrakis(trimethylsilyl)silane ($C_{12}H_{36}Si_5$, Stream Chemicals Co.), which was used as the doping

component (Figure 1a). The introduction of fluorine-containing compounds into the growth system leads to the reduction of the content of NV in NDs.[15,16,18] Detonation NDs were introduced into the growth medium as seeds in the HPHT reaction to obtain higher yields. This carbon and silicon source mixture was cold-pressed as a tablet (5 mm diameter and 4 mm height) and placed into a graphite container, which simultaneously served as a heater for the high-pressure Toroid-type apparatus. The HPHT growth comprised the following steps: (1) reaching high pressure (8.0 GPa) at room temperature, (2) heating to high temperature (~1400 °C) for diamond formation, and (3) an isothermal exposure for short time (3 s). Then the temperature decreased to room temperature, while the pressure remained high. Applied conditions triggered NDs formation inside the initial tablet of pressed components. Five batches were synthesized under the same conditions and combined to maximize the amount of NDs powder. Steel ball milling was applied to break obtained tablets to micro- and nanoparticles for subsequent chemical cleaning. A primary cleaning with $HNO_3$:$HClO_4$:$H_2SO_4$ at 230 °C for 5 h generated a powder, which was then neutralized with $NH_4OH$ buffer, washed, and dried as depicted in Figure 1a.

Scanning and transmission electron microscopy (SEM and TEM, Figure S1 and S2) showed the formation of diamonds of nano- and micro-size with cuboctahedral shape. The photoluminescence (PL) measurements demonstrated a very sharp and clear spectrum of SiV (Figure 1c) when $C_{10}F_8$ was applied as a starting material. In contrast, NDs synthesized without $C_{10}F_8$ have shown strong NV and SiV emissions in their PL spectra (Figure S3). The demonstrated HPHT ND-SiV synthesis offers several distinct advantages: (1) no metal catalyst is employed that could remain as impurities in the NDs, (2) no post-processing of irradiation or annealing is required to activate the color centers, and (3) the method is scalable up to several milligram quantities, which would allow extensive cell studies with the same batch.

Surface cleaning and oxidization were done by combining strong acid treatment ($HNO_3$-$H_2SO_4$-$HClO_4$, ratio 1:1:1, at 90 °C for 8 h) with sonication (Figure 1a). We obtained 5 mg of stable ND-SiV suspension in water without clusters with polar carboxylic acid surface groups for stable fluorescence[19] and further chemical modifications.[20] The average hydrodynamic radius of fluorescent ND-SiV of 62 ± 5 nm (Figure 1d) was initially determined by fluorescence correlation spectroscopy (FCS)[21] in water. FCS experiment demonstrated the lack of NDs clusters. Subsequently, dynamic light scattering measurement (DLS) showed the size distribution of NDs radius as 52.3 ± 3.6 nm (Figure 2f) with a polydispersity index (PDI) of 0.16 (Figure S7). FCS method detects only fluorescent nanoparticles, whereas DLS technique measures all presented NDs. This can explain the small difference in NDs size measured by FCS and DLS methods. Besides, there is a difference in the polydispersity averaging index of FCS and DLS measurements.[22] After the acid treatment, the ND-SiV exhibited negative zeta-potential with single peak distribution ($\zeta$ = -29.33 mV, Figure 2g and S8-S10).

The application of ND-SiV for cellular studies requires surface coating that imparts colloidal stability in cell media and allows cellular uptake via endocytosis and trafficking to cellular compartments as well as low cellular toxicity. We have previously reported the conversion of proteins into biocompatible NDs surface coatings that have been applied *in vitro* and *in vivo*.[23] In the current work, the surface coating was based on the abundant serum protein – human serum albumin (HSA) that was chemically modified by reacting ethylenediamine groups with the carboxylic acid surface groups of aspartic acid and glutamic acid residues yielding cationic HSA (cHSA, cationazation) (see Figure 2a and Figure S4).[23-25] cHSA with multiple additional amino groups provides multiple positive net charges, which are required for the subsequent formation of stable complexes with a negatively charged surface of ND-SiV by electrostatic interactions.

Hydrophilic polyethylene glycol (PEG) chains (molecule weight 2000 Da) were conjugated to cHSA to improve the colloidal stability of the modified protein polymer as well as the coated ND-SiV (cHSA-PEO, PEGlytion). Next, the polypeptide backbone of cHSA-PEO was unfolded by the reduction of the disulfide bridges. The generated free sulfhydryl groups were capped with N-(2-aminoethyl)maleimide to obtain the stable single-chain biopolymer (dcHSA-PEO, denaturation). The synthesis and characterization of the biopolymer dcHSA-PEO have been reported previously[23] and are included in the SI (Figure S11 and Figure S12).

ND-SiV diluted in boric acid buffer (0.05 mg $mL^{-1}$, 20 mL, pH = 8.4) were mixed with dcHSA-PEO (0.2 mg $mL^{-1}$, 20 mL) via titration addition, and coating proceeded by electrostatic absorption overnight. After ultrafiltration (cutoff 30 KD) and centrifugation (17000 RPM, 30 min, 3 times), the ND mixture was concentrated and unbound dcHSA-PEO biopolymer was removed. About 1 mg (50% yield) coated ND-SiV were obtained, termed $ND_{SiV}$-polymer. Figure 2b shows the aberration-corrected high-resolution TEM (AC-HRTEM) image of $ND_{SiV}$-polymer in $[0\bar{1}1]$ projection. The $ND_{SiV}$-polymer particles were highly crystalline exhibiting sharp edges along the main crystallographic orientations. In the magnified image (Figure 2c), the (111) and (022) lattice planes of diamond were clearly resolved. Residual amounts of amorphous and non-diamond nanoparticles were also observed via AC-HRTEM (Figure S5), which could not be removed by the acid processing. However, the X-ray diffraction patterns (XRD) of the ND-SiV raw material indicated the typical diamond spectrum with reflections at (111) and (220) (Figure S6).

A uniform and discrete distribution of $ND_{SiV}$-polymer was observed by TEM (Figure 2d), with an average radius of 31.6 nm (histogram in Figure 2e) by analyzing 108 NDs in the TEM image. After polymer encapsulation, DLS measurements revealed a hydrodynamic radius of $ND_{SiV}$-

polymer in the water of about 63.6 ± 5.3 nm (PDI = 0.1) corresponding to an increase of about 11 nm due to the polymer shell (Figure 2f). The $ND_{SiV}$-polymer appeared colloidally stable also in phosphate-buffered saline (PBS, pH = 7.4), and the radius increased only slightly to 70nm (PDI = 0.08, DSL measurements). The surface charges of $ND_{SiV}$-polymer were positive ($\zeta$ = 21.3 mV) due to the presence of the polycationic biopolymer dcHSA-PEO. Nanoparticle surface coatings with positive net charges are considered beneficial to facilitate cellular uptake by interactions with negatively charged cell membranes (Figure 2f and g).[18, 23]

The $ND_{SiV}$-polymer was applied for live-cell imaging in HeLa cells used as a model cell line. $ND_{SiV}$-polymer (0.02 mg $mL^{-1}$) was incubated for 24 h to enable cellular uptake. The efficient cellular uptake into HeLa cells was recorded by confocal laser scanning microscopy (CLSM). In a previous study, ND-SiV powder prepared by the CVD method was directly incubated with cells[26] without stabilizing surface modifications. In this case, even after several days of incubation, only cell membrane labeling was observed. In our work, $ND_{SiV}$-polymer was homogeneously distributed inside the cell (Figure 3a and S13). Due to the high index of refraction, these $ND_{SiV}$-polymer act as strong light scatterers allowing to distinguish NDs from background fluorescence of HeLa cells, which proved to be very helpful for further multiple stained bioimaging. According to Figure 3a, the images taken in the reflection mode of $ND_{SiV}$-polymer showed a good localization match with the $ND_{SiV}$-polymer fluorescence images (colocalization coefficient 0.6), indicating that most NDs contained SiV centers. The non-overlapping portion was attributed to a small fraction of NDs lacking SiV centers since the reflection imaging depicts all ND particles, and fluorescence imaging shows only NDs with color centers. Also, in some small ND-SiV, SiV might blink and bleach, the mechanism responsible for that has not yet been fully understood.[27] Furthermore, a time series scan was processed to evaluate the photostability of

$ND_{SiV}$-polymer. Some of the fluorescent points bleached after three scanning sweeps (Figure S14a), but the remaining emitters revealed high stability (Figure S14b) suitable for cellular imaging and nanoparticle monitoring.

HeLa cells incubated with $ND_{SiV}$-polymer were placed under a home-built scanning confocal microscope for cell imaging (Figure 3b). The cell culture medium was replaced with a phenol red-free buffer to avoid additional fluorescence. The excitation was done by a laser at 532 nm with the power of 200 μW (measured before the objective). The fluorescence was observed simultaneously by two different detection channels. Channel 1 with a long-pass filter detected the light with a wavelength longer than 575 nm (Figure 3b, (i, iii)). Channel 2 had a band-pass filter to register the light in the range of 720-760 nm, which corresponds to SiV fluorescence. The initial images of HeLa cells incubated with $ND_{SiV}$-polymer are presented in Figure 3b (i, ii). In channel 1 (Figure 3b (i)), we observed SiV together with the autofluorescence of the cell. To prove the presence and position of $ND_{SiV}$-polymer only, channel 2 was successfully used (Figure 3b (ii)). Cell autofluorescence is very weak, therefore, the CellMask green dye was added to the sample for better cell visualization (Figure 3b (iii, iv)). The signal from CellMask green is a few orders of magnitude higher than that from SiV due to the high number of dye molecules in the focal spot (Figure 3b (iii)). However, it does not disturb the image in channel 2, where the SiV image (Figure 3b (iv)) is similar to the one obtained before adding membrane dye. These experiments proved the usability of ND-SiV for dual-color live-cell imaging because the sharp NIR ZPL emission of ND-SiV can be easily separated from many dyes and drugs.

As a preliminary attempt, we have tracked 135 single fluorescent points for 90 min each with refocus intervals of 40 s. The representative trajectories of two different points are shown in Figure 4a. They are accomplished by the fluorescence intensities of $ND_{SiV}$-polymer during the tracking

experiments (Figure 4b). The presence of SiV centers is proven by spectral measurements (Figure 4c). We deduced that in this experiment, the tracked points contain ~5 SiV (Point 1) and ~4 SiV (Point 2) by comparing it with the saturated fluorescence intensity (~103 kcounts/s) of a single SiV reported in the literature,[28] which was measured with similar experiment configuration (processed under similar fluorescence collection efficiencies). The fluorescence intensities of tracked $ND_{SiV}$-polymer remained relatively stable, with low fluctuations in the fluorescence intensity of Point 1. These fluctuations could be attributed to the fast diffusion from the focal point of the objective, or a rotational movement induced by different excitation efficiencies leading to fluorescence intensity changes during tracking. In general, we did not observe a significant decrease in the fluorescence intensities indicating that $ND_{SiV}$-polymer allow long-term cellular tracking studies.

We have reported live-cell dual-color imaging and tracking applications of NDs containing only SiV centers produced by the improved metal-catalyst-free HPHT method. In this way, NIR emitters were obtained with a single sharp emission peak. These ND-SiV were coated with a protein-derived biopolymer that remains their colloidal stability in water solution as well as cell media. NIR fluorescence, sharp ZPL, and high fluorescence stability were key characteristics of these nanoemitters qualifying them for living cell imaging and tracking. For the first time, HPHT ND-SiV were observed in dual-color imaging and tracking for up to 90 min inside living cells without photobleaching. We believe that ND-SiV represent a powerful tool for intracellular imaging[29] and tracking.[30] Moreover, ND-SiV will offer great opportunities for intracellular real-time all-optical temperature sensing due to the temperature-dependent ZPL shift of SiV.[10] Since NDs can be also used for drug delivery,[23] a combination of all demonstrated properties of the ND-SiV system paves the way towards theranostic applications.

FIGURES.

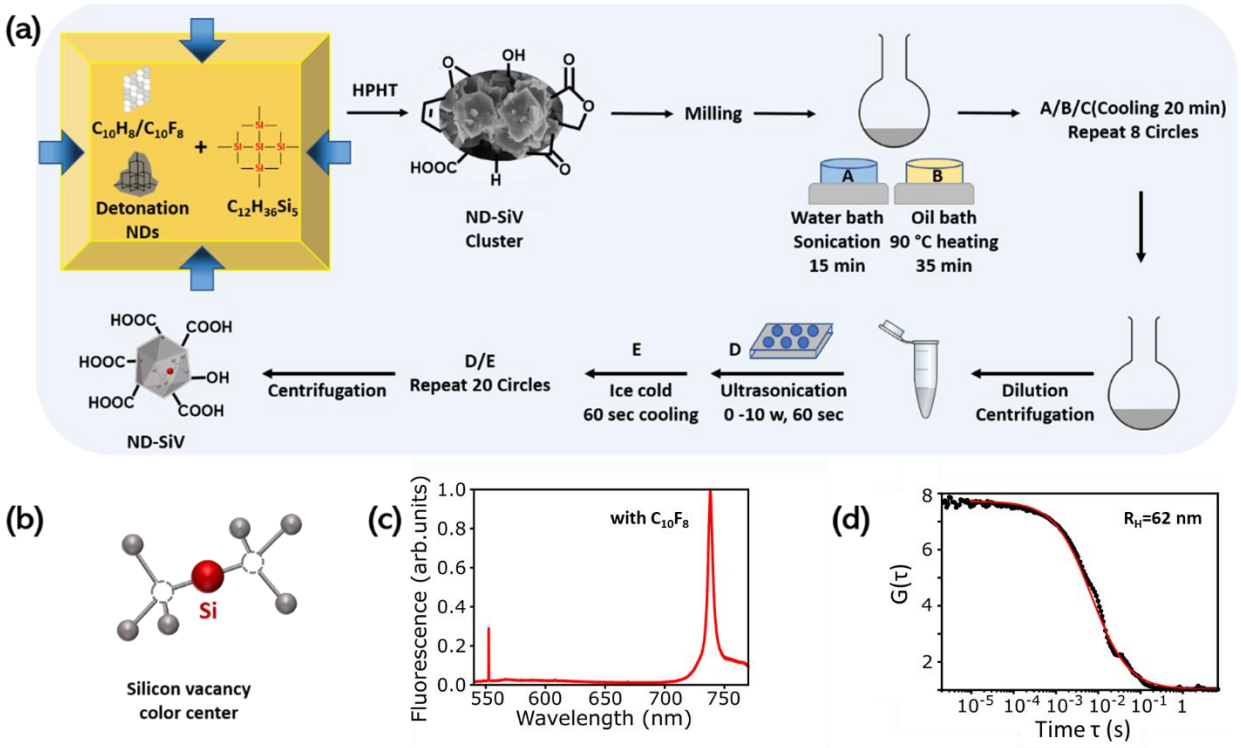


**Figure 1.** (a) Schematic presentation of ND-SiV HPHT synthesis and treatment. Raw ND-SiV clusters were obtained and imaged by scanning electron microscopy (full image in Figure S2). (b) Atomic structure of SiV center in the diamond lattice. (c) PL spectra of HPHT ND-SiV synthesized with $C_{10}F_8$. (d) FCS autocorrelation curves of ND-SiV in water solution.

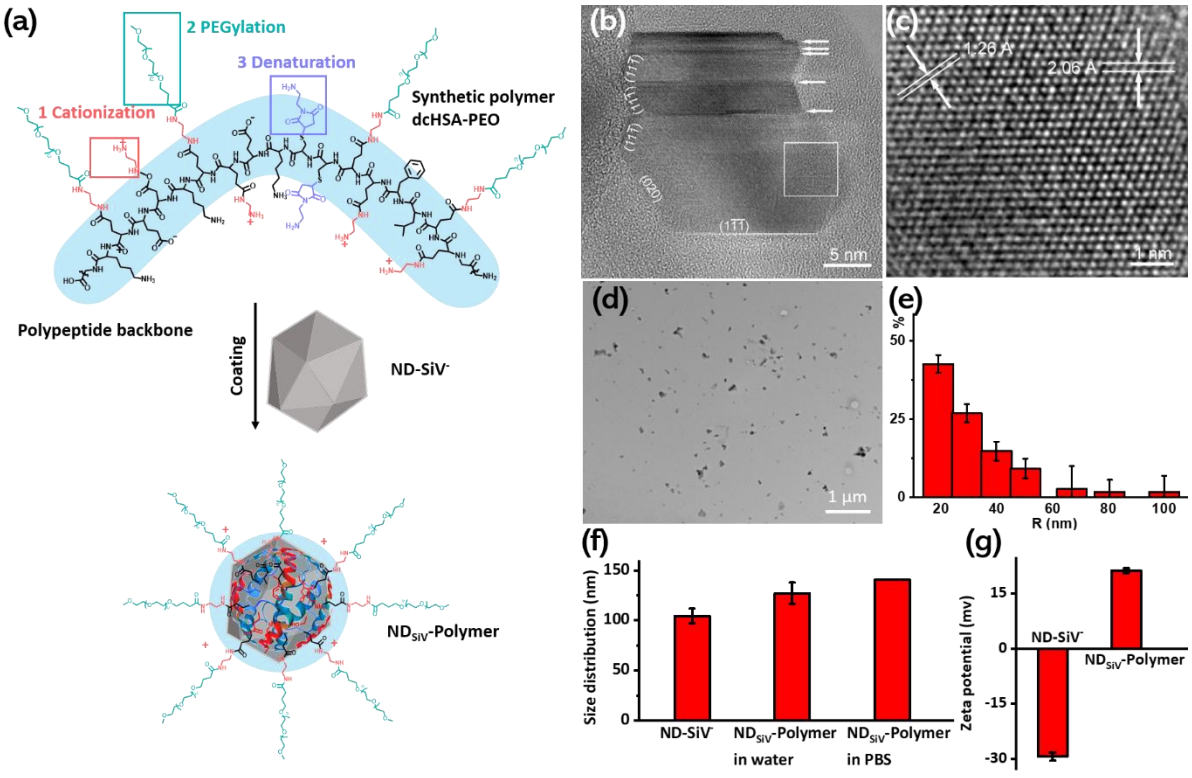


**Figure 2.** $ND_{SiV}$-polymer preparation and characterization. (a) ND-SiV modification by the biopolymer dcHSA-PEO coating. (b) [0$\bar{1}$1] AC-HRTEM image of ND-SiV consisting of crystalline domains separated by twin boundaries (marked by arrows). (c) Magnified image from the boxed region in (b), showing the distances ***d*** between the diamond lattice planes: (111) (d=2.06 Å) and (022) (***d***=1.26 Å). (d) TEM image of coated $ND_{SiV}$-polymer. Small clusters can be observed from the TEM images, but most of the NDs are discrete nanoparticles. (e) Histogram of NDs radius, quantification of 108 NDs from (d). (f) DLS radius of ND-SiV in water and $ND_{SiV}$-polymer in water and PBS buffer. (g) Zeta-potential of ND-SiV and $ND_{SiV}$-polymer.

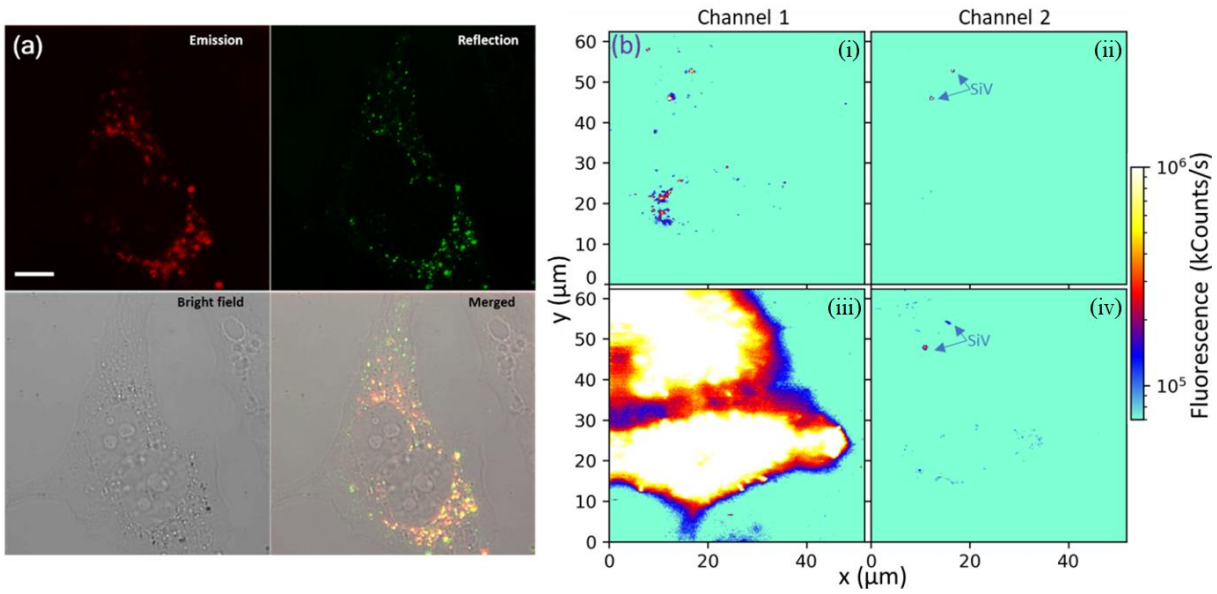


**Figure 3.** $ND_{SiV}$-polymer for dual-color cell imaging. (a) CLSM cell images showing efficient cell uptake. Emission and reflection channels demonstrated very good colocolization ($\lambda_{ex}$ = 561 nm, $\lambda_{em}$ = 700 – 758 nm, $\lambda_{re}$ = 556 – 566 nm, scale bar = 10 µm). (b) The fluorescence cell images obtained by home-built scanning confocal microscope ($\lambda_{ex}$ = 532 nm) with two detection channels (1 – $\lambda_{em}$ = 575 nm and longer, 2 – $\lambda_{em}$ = 720-760 nm).

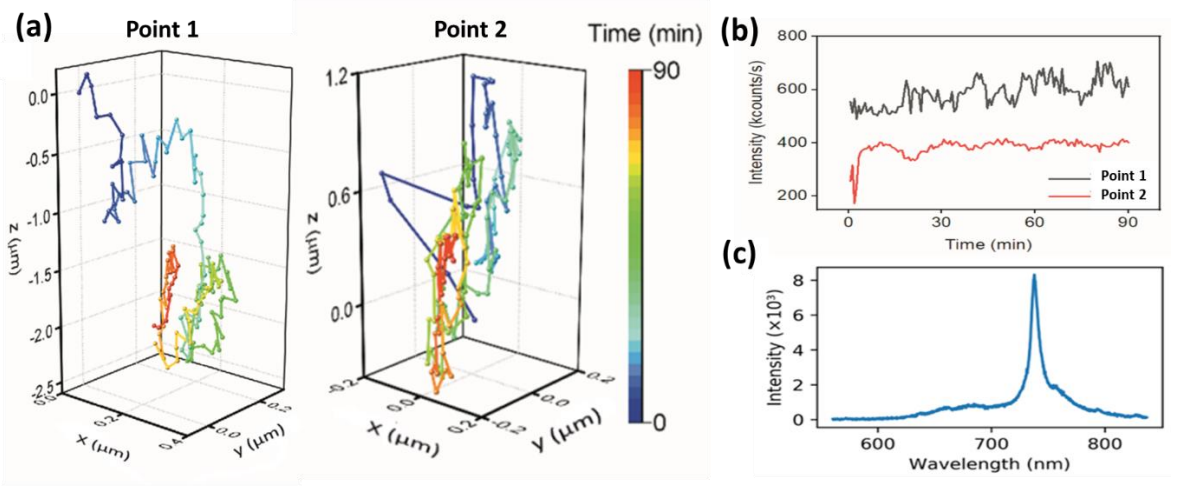

**Figure 4.** $ND_{SiV}$-polymer for cellular tracking. (a) The trajectory of two different NDs-SiV spots (point 1 and point 2) tracked in intracellular space. (b) Fluorescence intensity of the tracked NDs-SiV spots. (c) SiV spectra were observed from the NDs-SiV during the tracking measurements.

**Supporting Information**. The Supporting Information is available free of charge on the ACS Publications website at XXX

AUTHOR INFORMATION

**Corresponding Author**

* anna.ermakova@mpip-mainz.mpg.de *fedor.jelezko@uni-ulm.de * weil@mpip-mainz.mpg.de

**Present Addresses**

†If an author's address is different than the one given in the affiliation line, this information may be included here.

**Author Contributions**

W. Liu, A. Ermakova, and T. Weil initiated the draft. V. N. Agafonov, V. A. Davydov and R. Uzbekov contributed to the HPHT ND-SiV synthesis and raw material characterization. H. Qi and U. Kaiser contributed to the HRTEM characterization. W. Liu and T. Weil contributed to the ND-SiV acid treatment, $ND_{SiV}$-polymer preparation and characterization, bioimaging in CLSM microscopy (Zeiss 710) and cell experiments. A. Ermakova, Y. Liu and F. Jelezko contributed to the dual-color live-cell bioimaging, intracellular tracking and spectral measurements in home-built

scanning confocal microscopy and are responsible for the photo physics. T. Lasser contributed writing the manuscript and interpreting experimental data. The manuscript was written through contributions of all authors. The manuscript was written through contributions of all authors. All authors have given approval to the final version of the manuscript.

**Funding Sources**

This work has been supported by the ERC Synergy grant no. 319130-BioQ. V. A. Davydov thanks the Russian Foundation for Basic Research (Grant No. 18-03-00936) for financial support. T.W. and F.J. acknowledge funding by the Deutsche Forschungsgemeinschaft (DFG, German Research Foundation) – Projektnummer 316249678 – SFB 1279 (C01, C04) and Projektnummer 318290668 – SPP 1923.

ACKNOWLEDGMENT

W. Liu acknowledges Dr. Todd Zapata (Max Planck Institute for Polymer Research, Germany) and Dr. Qiong Chen (Hunan Normal University, China) for very helpful discussion.

ABBREVIATIONS

CCR2, CC chemokine receptor 2; CCL2, CC chemokine ligand 2; CCR5, CC chemokine receptor 5; TLC, thin layer chromatography.

REFERENCES

[1] Yu, S.-J.; Kang, M.-W.; Chang, H.-C.; Chen, K.-M.; Yu, Y.-C., Bright Fluorescent Nanodiamonds: No Photobleaching and Low Cytotoxicity. *Journal of the American Chemical Society* **2005,** *127* (50), 17604–17605

[2] Tzeng, Y. K.; Faklaris, O.; Chang, B. M.; Kuo, Y.; Hsu, J. H.; Chang, H. C., Superresolution Imaging of Albumin-Conjugated Fluorescent Nanodiamonds in Cells by Stimulated Emission Depletion. *Angewandte Chemie International Edition* **2011,** *50* (10), 2262-2265.

[3] Hsiao, W. W.-W.; Hui, Y. Y.; Tsai, P.-C.; Chang, H.-C., Fluorescent Nanodiamond: A Versatile Tool for Long-Term Cell Tracking, Super-Resolution Imaging, and Nanoscale Temperature Sensing. *Accounts of Chemical Research* **2016,** *49* (3), 400-407.

[4] Ermakova, A.; Pramanik, G.; Cai, J.-M.; Algara-Siller, G.; Kaiser, U.; Weil, T.; Tzeng, Y.-K.; Chang, H.; McGuinness, L.; Plenio, M., Detection of a few metallo-protein molecules using color centers in nanodiamonds. *Nano letters* **2013,** *13* (7), 3305-3309.

[5] Chang, Y.-R.; Lee, H.-Y.; Chen, K.; Chang, C.-C.; Tsai, D.-S.; Fu, C.-C.; Lim, T.-S.; Tzeng, Y.-K.; Fang, C.-Y.; Han, C.-C.; Chang, H.-C.; Fann, W., Mass production and dynamic imaging of fluorescent nanodiamonds. *Nature Nanotechnology* **2008**, *3*, 284-288.

[6] Doherty, M. W.; Manson, N. B.; Delaney, P.; Jelezko, F.; Wrachtrup, J.; Hollenberg, L. C., The nitrogen-vacancy colour center in diamond. *Physics Reports* **2013,** *528* (1), 1-45.

[7] Vlasov, I. I.; Shiryaev, A. A.; Rendler, T.; Steinert, S.; Lee, S.-Y.; Antonov, D.; Vörös, M.; Jelezko, F.; Fisenko, A. V.; Semjonova, L. F.; Biskupek, J.; Kaiser, U.; Lebedev, O. I.; Sildos, I.; Hemmer, P. R.; Konov, V. I.; Gali, A.; Wrachtrup, J., Molecular-sized fluorescent nanodiamonds. *Nature Nanotechnology* **2013,** *9*, 54-58.

[8] Weissleder, R., A clearer vision for in vivo imaging. *Nature Biotechnology* **2001,** *19*, 316-317.

[9] Sajedi, S.; Sabet, H.; Choi Hak, S., Intraoperative biophotonic imaging systems for image-guided interventions. *Nanophotonics* **2018,** *8* (1), 99-116.

[10] Nguyen, C. T.; Evans, R. E.; Sipahigil, A.; Bhaskar, M. K.; Sukachev, D. D.; Agafonov, V. N.; Davydov, V. A.; Kulikova, L. F.; Jelezko, F.; Lukin, M. D., All-optical nanoscale thermometry with silicon-vacancy centers in diamond. *Applied Physics Letters* **2018,** *112* (20), 203102.

[11] Grudinkin, S. A.; Feoktistov, N. A.; Baranov, M. A.; Smirnov, A. N.; Davydov, V. Y.; Golubev, V. G., Low-strain heteroepitaxial nanodiamonds: fabrication and photoluminescence of silicon-vacancy colour centers. *Nanotechnology* **2016,** *27* (39), 395606.

[12] Vlasov, I. I.; Barnard, A. S.; Ralchenko, V. G.; Lebedev, O. I.; Kanzyuba, M. V.; Saveliev, A. V.; Konov, V. I.; Goovaerts, E., Nanodiamond Photoemitters Based on Strong Narrow-Band Luminescence from Silicon-Vacancy Defects. *Advanced Materials* **2009,** *21* (7), 808-812.

[13] Shenderova, O. A.; Shames, A. I.; Nunn, N. A.; Torelli, M. D.; Vlasov, I.; Zaitsev, A., Review Article: Synthesis, properties, and applications of fluorescent diamond particles. *Journal of Vacuum Science & Technology B* **2019,** *37* (3), 030802.

[14] Davydov, V. A.; Rakhmanina, A. V.; Agafonov, V.; Narymbetov, B.; Boudou, J. P.; Szwarc, H., Conversion of polycyclic aromatic hydrocarbons to graphite and diamond at high pressures. *Carbon* **2004,** *42* (2), 261-269.

[15] Davydov, V. A.; Rakhmanina, A. V.; Lyapin, S. G.; Ilichev, I. D.; Boldyrev, K. N.; Shiryaev, A. A.; Agafonov, V. N., Production of nano- and microdiamonds with Si-V and N-V

luminescent centers at high pressures in systems based on mixtures of hydrocarbon and fluorocarbon compounds. *JETP Letters* **2014,** *99* (10), 585-589.

[16] Davydov, V. A.; Agafonov, V.; Khabashesku, V. N., Comparative Study of Condensation Routes for Formation of Nano- and Microsized Carbon Forms in Hydrocarbon, Fluorocarbon, and Fluoro-Hydrocarbon Systems at High Pressures and Temperatures. *The Journal of Physical Chemistry C* **2016,** *120* (51), 29498-29509.

[17] Choi, S.; Leong, V.; Davydov, V. A.; Agafonov, V. N.; Cheong, M. W. O.; Kalashnikov, D. A.; Krivitsky, L. A., Varying temperature and silicon content in nanodiamond growth: effects on silicon-vacancy centers. *Scientific Reports* **2018,** *8* (1), 3792.

[18] Davydov, V. A.; Rakhmanina, A. V.; Agafonov, V.; Khabashesku, V. N., On the nature of simultaneous formation of nano- and micron-size diamond fractions under pressure–temperature-induced transformations of binary mixtures of hydrocarbon and fluorocarbon compounds. *Carbon* **2015,** *90*, 231-233.

[19] Nagl, A.; Hemelaar, S. R.; Schirhagl, R., Improving surface and defect center chemistry of fluorescent nanodiamonds for imaging purposes—a review. *Analytical and Bioanalytical Chemistry* **2015,** *407* (25), 7521-7536.

[20] Osswald, S.; Yushin, G.; Mochalin, V.; Kucheyev, S. O.; Gogotsi, Y., Control of sp2/sp3 Carbon Ratio and Surface Chemistry of Nanodiamond Powders by Selective Oxidation in Air. *Journal of the American Chemical Society* **2006,** *128* (35), 11635-11642.

[21] Koynov, K.; Butt, H.-J., Fluorescence correlation spectroscopy in colloid and interface science. *Current Opinion in Colloid & Interface Science* **2012,** *17* (6), 377-387.

[22] Schaeffel, D.; Yordanov, S.; Staff, R. H.; Kreyes, A.; Zhao, Y.; Schmidt, M.; Landfester, K.; Hofkens, J.; Butt, H.-J.; Crespy, D.; Koynov, K., Fluorescence Correlation Spectroscopy in Dilute Polymer Solutions: Effects of Molar Mass Dispersity and the Type of Fluorescent Labeling. *ACS Macro Letters* **2015,** *4* (2), 171-176.

[23] Wu, Y.; Ermakova, A.; Liu, W.; Pramanik, G.; Vu, T. M.; Kurz, A.; McGuinness, L.; Naydenov, B.; Hafner, S.; Reuter, R.; Wrachtrup, J.; Isoya, J.; Förtsch, C.; Barth, H.; Simmet, T.; Jelezko, F.; Weil, T., Programmable Biopolymers for Advancing Biomedical Applications of Fluorescent Nanodiamonds. *Advanced Functional Materials* **2015,** *25* (42), 6576-6585.

[24] Wu, Y.; Eisele, K.; Doroshenko, M.; Algara-Siller, G.; Kaiser, U.; Koynov, K.; Weil, T., A Quantum Dot Photoswitch for DNA Detection, Gene Transfection, and Live-Cell Imaging. *Small* **2012,** *8* (22), 3465-3475

[25] Zhang, T.; Neumann, A.; Lindlau, J.; Wu, Y.; Pramanik, G.; Naydenov, B.; Jelezko, F.; Schüder, F.; Huber, S.; Huber, M.; Stehr, F.; Högele, A.; Weil, T.; Liedl, T., DNA-Based Self-Assembly of Fluorescent Nanodiamonds. *Journal of the American Chemical Society* **2015,** *137* (31), 9776-9779.

[26] Merson, T. D.; Castelletto, S.; Aharonovich, I.; Turbic, A.; Kilpatrick, T. J.; Turnley, A. M., Nanodiamonds with silicon vacancy defects for nontoxic photostable fluorescent labeling of neural precursor cells. *Optics Letters* **2013,** *38* (20), 4170-4173.

[27] Neu, E.; Agio, M.; Becher, C., Photophysics of single silicon vacancy centers in diamond: implications for single photon emission. *Optics Express* **2012,** *20* (18), 19956-19971.

[28] Liu, Y.; Chen, G.; Rong, Y.; McGuinness, L. P.; Jelezko, F.; Tamura, S.; Tanii, T.; Teraji, T.; Onoda, S.; Ohshima, T.; Isoya, J.; Shinada, T.; Wu, E.; Zeng, H., Fluorescence Polarization Switching from a Single Silicon Vacancy Colour Center in Diamond. *Scientific Reports* **2015,** *5*, 12244.

[29] Han, S.; Raabe, M.; Hodgson, L.; Mantell, J.; Verkade, P.; Lasser, T.; Landfester, K.; Weil, T.; Lieberwirth, I., High-Contrast Imaging of Nanodiamonds in Cells by Energy Filtered and Correlative Light-Electron Microscopy: Toward a Quantitative Nanoparticle-Cell Analysis. *Nano Letters* **2019,** *19* (3), 2178-2185.

[30] Hui, Y. Y.; Hsiao, W. W-W.; Haziza, S.; Simonneau, M.; Treussart, F; Chang, H.-C., Single particle tracking of fluorescent nanodiamonds in cells and organisms. *Current Opinion in Solid State and Materials Science* **2017,** *21* (1), 35-42.